AIAA AVIATION Forum
5-9 June 2017, Denver, Colorado
AIAA Atmospheric Flight Mechanics Conference

10.2514/6.2017-4209

Check for updates

Re-entry Trajectory Design using Pigeon Inspired Optimization

Gangireddy Sushnigdha* Ashok Joshi†

This paper presents the application of Pigeon Inspired Optimization (PIO) for designing a constrained entry trajectory of re-entry vehicles. Bank angle modulation is considered to be the primary control mechanism during the entry phase. Heading angle offset is reduced by using traditional bank reversal logic. The complete control profile determination problem is reduced to a single parameter search problem. The terminal conditions that are to be satisfied are part of the objective function and the path constraints are incorporated by penalty factor approach. Simulation results demonstrate the effectiveness of PIO algorithm over Particle swarm optimization (PSO) and Gravitational search algorithms (GSA).

Nomenclature

r	Radial distance from centre of the Earth to the vehicle
V	Velocity of vehicle relative to Earth
γ	Flightpath angle
ψ	Heading angle
θ	Longitude
ϕ	Latitude
s	Range to go
m	Mass
S_{ref}	Reference area
L	Aerodynamic lift acceleration
D	Aerodynamic lift acceleration
g_0	Acceleration due to gravity in
R_0	Radius of Earth
Ω	Angular velocity of Earth
C_L	Coefficient of lift
C_D	Coefficient of drag
ρ	Atmospheric density
$\dot{Q}$	Heat rate
a	Load factor
q	Dynamic pressure
$\dot{Q}_{max}$	Maximum allowable heat rate
a_{max}	Maximum allowable load factor
q_{max}	Maximum allowable dynamic pressure
e	Negative of specific mechanical energy
μ	Universal gravitational parameter
σ	Bank angle
σ_0	Initial bank angle
ψ_{LOS}	Azimuth angle
$\Delta\psi$	Heading error offset
χ	Crossrange parameter

*Research Scholar, Department of Aerospace Engineering, IIT Bombay, Mumbai, Maharashtra, 400076, India
†Professor, Department of Aerospace Engineering, IIT Bombay, Mumbai, Maharashtra, 400076, India, and Senior member AIAA

Copyright © 2017 by the American Institute of Aeronautics and Astronautics, Inc. All rights reserved.

Downloaded by BEIHANG UNIVERSITY on April 28, 2018 | http://arc.aiaa.org | DOI: 10.2514/6.2017-4209

t_f Final time of flight
N Population of the pigeons
D Dimension of the problem
k_{max} Maximum iterations
k_c Iteration corresponding to shift in operator
X_i Array containing position of the pigeons
V_i Array containing velocity of the pigeons
R Map and compass operator
k Current iteration
G Global best position of the pigeon
N_p Reduced population of the pigeons
X_c Centre of the pigeons
J Objective function

Subscript
i i th pigeon
0 Initial conditions
f Final conditions

Downloaded by BEIHANG UNIVERSITY on April 28, 2018 | http://arc.aiaa.org | DOI: 10.2514/6.2017-4209

I. Introduction

Re-entry phase is very crucial for any spacecraft, reusable launch vehicle, hypersonic gliding vehicles etc., that are returning from space to the Earth. These vehicles rely on entry trajectories to reach the destination safely. Usually entry trajectories are designed offline and stored onboard before the mission starts. Designing the entry trajectory is a challenging task as entry dynamics are highly nonlinear, uncertain and with limited control capability. Such trajectories are also required to be within the entry corridor that is formed by maximum allowable limits on heat rate, dynamic pressure and load factor.

Entry trajectory design is an optimal control problem whose solution is usually obtained through indirect and direct methods. Indirect methods are based on the Pontryagin minimum principle which leads to two point boundary value problem.[1] However, direct methods involve discretizing control time histories and/or state variable time history, thereby transforming the optimal control problem to a nonlinear programming problem (NLP).[2] Pseudospectral methods that fall under the category of direct method have been used extensively to solve trajectory optimization problems. Legendre pseudospectral method approach has been implemented for entry trajectory optimization by Tian and Qun Zong.[3] Other pseudospectral methods like Gauss, Radau, Chebyshev have been applied for generating entry trajectories by Jorris et al.,[4] K.Kalirajan et al.,[5] and Wei et al.,[6] respectively. However, pseudospectral methods have tuning issues, because of requirement of careful selection of basis functions and the number of collocation points.

Among the direct methods, evolutionary algorithms that mimic natural phenomena have gained popularity because of their simplicity in the problem formulation. Some of the popular algorithms are genetic algorithm (GA),[7] algorithms based on swarm intelligence like PSO,[8] ant-colony optimization.[9] Rahimi et al.,[10] have applied PSO to generate optimal trajectories for a spacecraft. In recent times, an evolutionary algorithm named PIO that mimics the homing behaviour of pigeons has been proposed by Duan.[11] Jiang et al.,[12,13] have implemented PSO and PIO to generate entry trajectories for hypersonic gliding vehicle using a simple formulation. They have considered few entry cases with short downrange to be travelled that have one or two bank reversals. In these problems the control formulation requires finding multiple parameters to get the complete control profile. However, there are no reported studies on application of PIO for long downrange missions. Therefore, in this paper, application of PIO has been demonstrated for the entry case that has long downrange, which is to be covered with one control parameter search operation. To reduce the order of the problem, the control variable, bank angle; has been parametrized to be linear with respect to energy. To show the effectiveness of PIO, simulation results have been compared with PSO and gravitational search algorithms (GSA).

II. Equations of motion

The re-entry vehicle gliding over a spherical, rotating Earth is considered to be a point mass. The 3-DOF entry dynamics of the vehicle are given below[14]

$$\dot{r} = V\sin\gamma \tag{1}$$

$$\dot{V} = -D - \frac{\sin\gamma}{r^2} + \Omega^2 r\cos\phi(\sin\gamma\cos\phi - \cos\gamma\sin\phi\cos\psi) \tag{2}$$

$$\dot{\theta} = \frac{V\cos\gamma\sin\psi}{r\cos\phi} \tag{3}$$

$$\dot{\phi} = \frac{V\cos\gamma\cos\psi}{r} \tag{4}$$

$$\dot{\gamma} = \frac{1}{V}\Big[L\cos\sigma + (V^2 - \frac{1}{r})(\frac{\cos\gamma}{r}) + 2\Omega V\cos\phi\sin\psi + \Omega^2 r\cos\phi(\cos\gamma\cos\phi + \sin\gamma\cos\psi\sin\phi\Big] \tag{5}$$

$$\dot{\psi} = \frac{1}{V}\Big[\frac{L\sin\sigma}{\cos\gamma} + \frac{V^2}{r}\cos\gamma\sin\psi\tan\phi - 2\Omega V(\tan\gamma\cos\psi\cos\phi - \sin\phi) + \frac{\Omega^2 r}{\cos\gamma}\sin\psi\sin\phi\cos\phi\Big] \tag{6}$$

$$\dot{s} = -V\cos\gamma/r \tag{7}$$

The differentiations in the equations of motion are with respect to dimensionless time $\tau = t/t_{scale}$, where $t_{scale} = \sqrt{\frac{R_0}{g_0}}$. All the above mentioned variables in the entry dynamics are dimensionless. r is the nondimensional distance from the Earth centre to the point mass O that is normalized by the radius of the Earth $R_0 = 6378.135km$. V is the Earth-relative velocity which is normalized by $V_{scale} = \sqrt{R_0 g_0}$, θ and ϕ are the longitude and latitude, γ is the flight-path angle and is positive when V is above the horizontal plane. ψ is the heading angle of the velocity vector, measured clockwise in the local horizontal plane from the north as shown in figure 1. s denotes the range to go (in radians, normalized by R_0) on the surface of the spherical Earth along the great circle connecting the current location of the vehicle and the site of the final destination.[14] g_0 is the acceleration due to gravity. Bank angle σ is defined as the clockwise positive rotation of the lift vector about the velocity vector. Ω is the dimensionless angular velocity of the Earth. L and D are nondimensional aerodynamic lift and drag accelerations normalized with $g_0 = 9.8m/s^2$ and are defined as

$$L = \frac{1}{2mg_0}\rho V^2 C_L S_{ref} \tag{8}$$

$$D = \frac{1}{2mg_0}\rho V^2 C_D S_{ref} \tag{9}$$

where m is the mass of the vehicle, S_{ref} is the surface area of the vehicle, ρ is the atmospheric density. C_L and C_D are the aerodynamic lift and drag coefficients that are functions of angle of attack and Mach number.

A. Choice of independent variable and calculation of final time of flight t_f

An energy like variable e is used as the independent variable for solving the trajectory optimization problem. e is defined as negative of the specific mechanical energy used in orbital mechanics as mentioned by Lu.[14]

$$e = \frac{\mu}{r} - \frac{V^2}{2} \tag{10}$$

where μ is gravitational parameter for the Earth, whose normalized value is 1. Eq. (11) shows that e is a monotonically increasing variable and is a function of radial distance and velocity. Therefore, the choice of e as an independent variable helps to consider the terminal conditions on r and V as a single constraint and these constraints can be achieved with better accuracy.

$$\frac{de}{d\tau} = DV > 0 \tag{11}$$

The equations of motion are integrated from initial energy e_0 to final energy e_f. e_f is calculated using the desired values of radial distance r^* and velocity V^*. Final time of flight t_f can be obtained as the part of the solution by including $\frac{d\tau}{de}$ in the equations of motion and integrating it from e_0 to e_f.

Downloaded by BEIHANG UNIVERSITY on April 28, 2018 | http://arc.aiaa.org | DOI: 10.2514/6.2017-4209

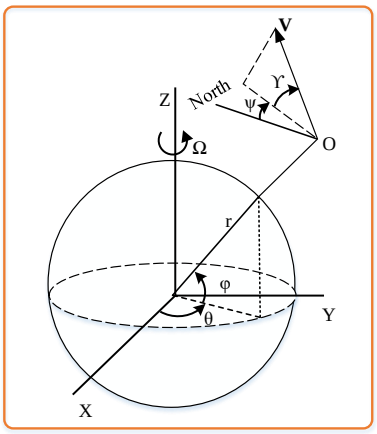

Figure 1. Nomenclature used in equations of motion.

Downloaded by BEIHANG UNIVERSITY on April 28, 2018 | http://arc.aiaa.org | DOI: 10.2514/6.2017-4209

III. Problem Statement

Trajectory optimization for entry vehicles involves finding the control profiles such that the resulting entry trajectory satisfies the path and terminal conditions. In this paper, bank angle is considered to be the only control variable. A fixed angle of attack profile has been considered. To solve this optimal control problem, bank angle has been parametrized with respect to energy e, as given below.

A. Control profile parametrization

The bank angle is considered to be a linear function of current energy e, based on piecewise linear approximation. Its magnitude is calculated from Eq. (12)

$$|\sigma(e)| = \sigma_0 + \frac{e - e_0}{e_f - e_0}(\sigma_f - \sigma_0) \tag{12}$$

where e_0 and e_f are energies at entry point and terminal points respectively. $\sigma_0 \geq 0$ is the parameter to be found that minimizes the applicable objective function J in Eq. (16). σ_f is the terminal bank angle. $\sigma_f = 60^\circ$ has been chosen for the simulations. The sign of bank angle is obtained from a bank reversal logic as described by Shen.[15]

1. *Bank reversal logic*

The main aim of bank reversal logic is to reduce the heading offset $\Delta\psi$ of the vehicle, defined below,

$$\Delta\psi = \psi - \psi_{LOS} \tag{13}$$

where ψ is the current actual heading angle and ψ_{LOS} is the azimuth angle at current location along great circle connecting the current location (θ, ϕ) and the final destination (θ_f, ϕ_f).

$$\psi_{LOS} = \sin^{-1}\left[\frac{\sin(\theta_f - \theta)\cos\phi_f}{\sin(s)}\right] \tag{14}$$

According to Shen,[15] heading error exhibits fast variations with respect to range as the vehicle approaches the TAEM phase. Hence, a crossrange parameter χ that varies almost linearly with range is defined in Eq. (15) to command the bank reversal.

$$\chi = \sin^{-1}[\sin(s)\sin\Delta\psi] \tag{15}$$

where, s is range to go as defined earlier. If the crossrange parameter χ exceeds the deadband $\Delta_{azmth}(V)$, the sign of bank angle is commanded to change to reduce $|\Delta\psi|$. $\Delta_{azmth}(V)$ is sometimes held constant or is varied as a linear function of velocity.

B. Objective Function

Trajectory optimization problem is stated as follows

$$Min\ J = |s(e_f) - s^*| + |r(e_f) - r^*| + |V(e_f) - V^*| \tag{16}$$

subject to constraints

$$\dot{Q} = 9.4369 \times 10^{-5} \sqrt{\rho} V^{3.15} \leq \dot{Q}_{max} \tag{17}$$

$$a = \sqrt{L^2 + D^2} \leq a_{max} \tag{18}$$

$$q = (g_0 R_0 \rho V^2)/2 \leq q_{max} \tag{19}$$

The maximum allowable limits on the heat rate $\dot{Q}$, dynamic pressure q and aerodynamic load factor a, form the boundaries of the entry corridor and hence appear as constraints to the optimal control problem.[14] The entry trajectory should be within the entry corridor. These constraints together form the path constraints. The entry trajectory should also satisfy the terminal conditions on altitude, velocity and range to go that are part of the objective function Eq. (16). In the objective function, "$*$" indicates the desired terminal states as defined by the Terminal Area Energy Management (TAEM) phase and the state variables are nondimensional as described in section II.

IV. Pigeon Inspired Optimization

PIO has been proposed by Duan[11,16] and has been successfully applied to various research problems. PIO is one of the methods based on swarm intelligence. It mimics the movement of a flock of pigeons who exhibit excellent homing behaviour. They navigate using two operators, called map and compass operator, landmark operator. Pigeons use map and compass operator during their initial phase of journey and later shift to landmark operator as they approach the destination.

A. Map and Compass Operator

Pigeons can locate themselves relative to their destination by being able to sense Earth's magnetic field. This is termed as map operator. They adjust their flying direction using altitude of the Sun, which is regarded as the compass operator. The basic algorithm is evolved as follows
Let the total population of the pigeons be N. Set the maximum number of iterations k_{max}. Define the dimension of the problem based on the number of unknown variables to be found. Let D denote the dimension of the problem. Define the search range for each dimension. Initial set of pigeons are randomly generated in the given search range. Position of the pigeon i is given by Eq. (20).

$$X_i = [x_{i1}, x_{i2}, ..., x_{iD}] \quad where\ i = 1, 2, 3...N \tag{20}$$

The velocity of the pigeon i is given by Eq. (21).

$$V_i = [v_{i1}, v_{i2}, ..., v_{iD}] \quad where\ i = 1, 2, 3...N \tag{21}$$

Each pigeons position represents a possible solution and corresponds to an objective function given in Eq. (16). In this operator, all the pigeons adjust their position and will try to follow the pigeon that corresponds to the best objective function value i.e minimum objective function. The position and velocities of the pigeons are updated in each iteration k as per following update logic

$$V_i(k) = V_i(k-1).e^{-Rk} + rand.\ (G(k-1) - X_i(k-1)) \tag{22}$$

$$X_i(k) = X_i(k-1) + V_i(k) \tag{23}$$

where $G(k-1)$ is the position of the pigeon corresponding to the best objective function achieved so far. $rand$ is random number in [0,1]. R is the map and compass operator. The term $V_i(k-1).e^{-Rk}$ gives the pigeons former flying direction. Figure 2, describes the steps for executing map and compass operator.

Downloaded by BEIHANG UNIVERSITY on April 28, 2018 | http://arc.aiaa.org | DOI: 10.2514/6.2017-4209

Downloaded by BEIHANG UNIVERSITY on April 28, 2018 | http://arc.aiaa.org | DOI: 10.2514/6.2017-4209

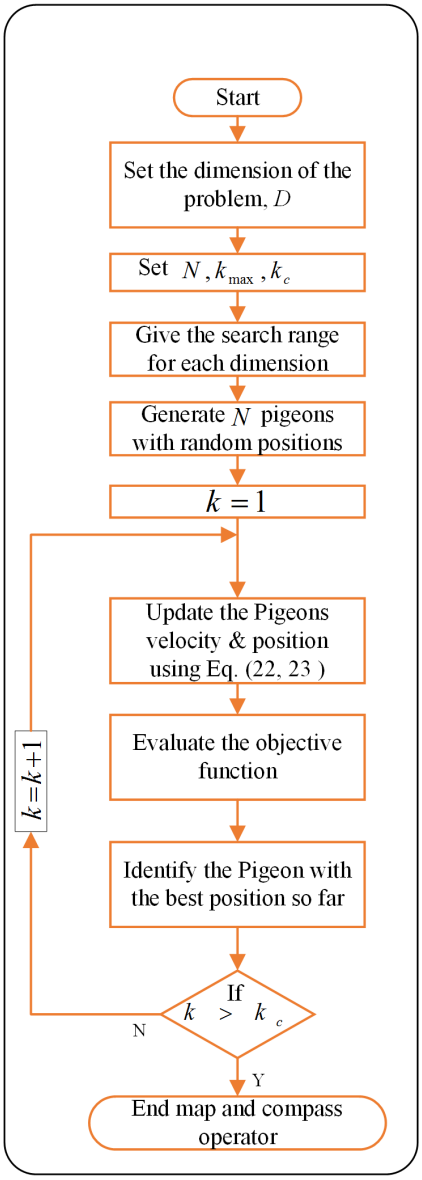

Figure 2. Flowchart for map and compass operator

B. Landmark operator

As pigeons approach their destination, they use landmark operator. Few pigeons can identify the landmarks and can fly directly to their destinations. The remaining pigeons follow them and reach the destination. Let k_c be the iteration number that indicates the shift in the operator. k_c is chosen to be less than k_{max}. When the iteration k exceeds k_c, landmark operator is initiated. In this operator, half of the pigeons with positions nearer to $G(k-1)$ are selected. The centre of these pigeons is found using Eq. (24).

$$X_c(k) = \frac{\sum_{N_p(k)} X_i(k-1).fitness(X_i(k-1))}{N_p(k) \sum_{N_p(k)} fitness(X_i(k-1))} \tag{24}$$

where $fitness()$ is the objective function value corresponding to the given pigeons position and N_p is the current reduced population as given below

$$N_p(k) = \frac{N_p(k-1)}{2} \tag{25}$$

Using $X_c(k)$, the positions of the pigeons is updated as follows

$$X_i(k) = X_i(k-1) + rand.\ (X_c(k) - X_i(k-1)) \tag{26}$$

In the landmark operator, pigeons that are not familiar with the landmarks, adjust their positions and follow the centre of the pigeons that are familiar with the landmarks. Finally, at the end of iterations pigeon corresponding to minimum objective function value will be the pigeon with best position. Flowchart describing the landmark operator is in figure 3. PIO algorithm as applied to the current problem is presented in the flowchart discussed in figure 4.

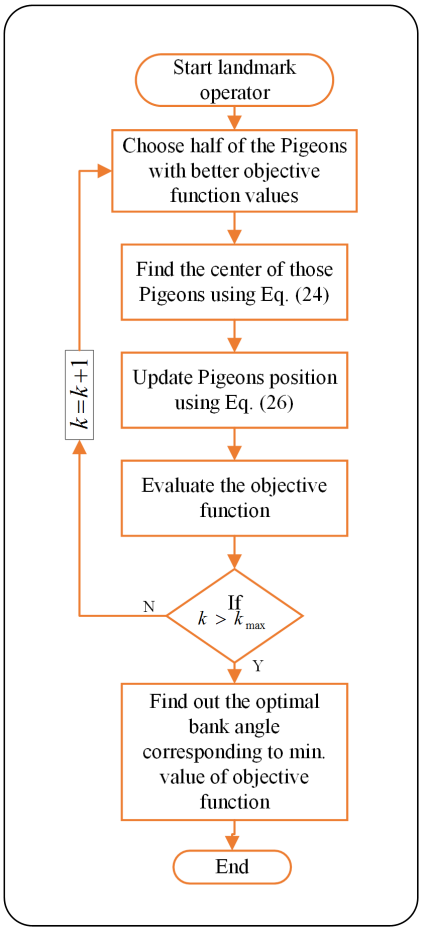

Figure 3. Flowchart for landmark operator

Downloaded by BEIHANG UNIVERSITY on April 28, 2018 | http://arc.aiaa.org | DOI: 10.2514/6.2017-4209

C. Constraints handling mechanism

The path constraints are handled by adding a high penalty factor to the objective function J, whenever they are violated. The presence of constraints further reduces the search space. If the maximum heat rate corresponding to a pigeon i violates the constraint, then the corresponding objective function J_i is given a high penalty. $J_i = 100000000$ has been considered for the simulations. Thus, this pigeon i is not eligible to become the pigeon with the best objective function.

Downloaded by BEIHANG UNIVERSITY on April 28, 2018 | http://arc.aiaa.org | DOI: 10.2514/6.2017-4209

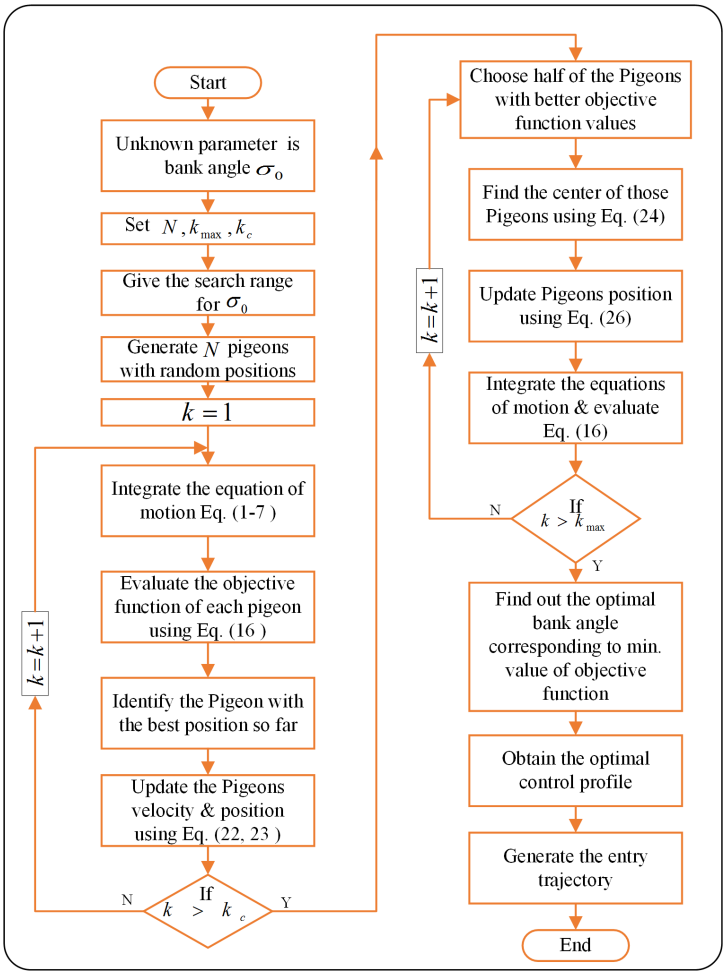

Figure 4. Flowchart of PIO for solving entry trajectory optimization problem

V. Simulation Results

Trajectory optimization using PIO has been applied to Common aero vehicle (CAV-H) with high L/D ratio. The aerodynamic coefficient data is given by Phillips.[17] A fixed angle of attack profile with Mach number is considered from Ping Lu.[14] The initial conditions used for the simulation are given in table 1 and the desired terminal conditions are in table 2. The path constraints considered for the simulation are $\dot{Q}_{max} = 7.5MW/m^2$, $q_{max} = 100kPa$ and $a_{max} = 2.3g$. These values are broadly based on the guidelines provided in Chen.[20] The longitude and latitude of the final destination are $\theta_f = 65.7\,\text{deg}$, $\phi_f = 31.6\,\text{deg}$. During the initial phase of entry, the bank angle σ is considered to be zero, till the vehicle attains a load factor greater than $1.5184m/s^2$. This is because the vehicle is at higher altitudes where the density is very small, this results in zero lift irrespective of the presence of bank angle. The velocity dependent deadband $\Delta_{azmth}(V)$ that has been considered for bank reversal is as given in Eq. (27). This bank reversal logic has resulted in final heading offset $|\Delta\psi(t_f)| < 5\,\text{deg}$.

$$\Delta_{azmth} \begin{cases} = 2\,\text{deg}, V \geq 6000m/s \\ = 3\,\text{deg}, V_2 < V < 6000m/s \\ = 3 - 0.1\left(\dfrac{V - V_2}{V_3 - V_2}\right) deg, V_3 \leq V \leq V_2 \\ = 0.1\,\text{deg}, V < V_3 \end{cases} \tag{27}$$

where $V^* = 2000\text{m/s}$, $V_2 = V^* + 1000$ and $V_3 = V^* + 200$ The parameters required for simulating PIO

Table 1. Initial entry conditions[21]

r_0 (km)	V_0 (m/s)	θ_0 (deg)	ϕ_0 (deg)	γ_0 (deg)	ψ_0 (deg)	s_0 (nm)
121.52+R_0	7400	-72.42	38.99	-1	35	6000

Table 2. Final conditions to be acheived[21]

r^* (km)	V^* (m/s)	s^* (nm)	$\Delta\psi_f \leq$ (deg)
28+R_0	2000	50	$\pm$ 10

algorithm are set as $N = 20$, $k_{max} = 25$, $D = 1$, $k_c = 15$, $R = 0.2$. The dimension of the problem is $D = 1$, as σ_0 is the only parameter to be found. The range of search space for σ_0 is given as $|\sigma_{min}| = 0°$ and $|\sigma_{max}| = 90°$.

A. Performance comparison

The results of PIO are compared with Particle swarm optimization and Gravitational Search algorithm (GSA).[18] These algorithms have the same initialization mechanisms. For comparison, the maximum number of iterations and the population of agents are considered to be same in all the three optimization algorithms. All the three algorithms have been run each 5 times. Comparative results have been displayed in the table 3. From the table, PIO shows the minimum objective function value with a mean of 0.00076071. Figure 5 shows the comparative curves corresponding to the best objective functions mentioned in the table 3. From figure 5, it can be concluded that PIO converges quickly to the minimum objective function value in lesser number of iterations as compared to PSO and GSA.

Table 3. Comparative results

Algorithms	Best objective function	Best parameter (Bank angle deg)	Mean objective function
PIO	0.0007607	71.62246	0.000760
PSO	0.0018434	71.59842	0.00789
GSA	0.0101234	71.41737	0.14902

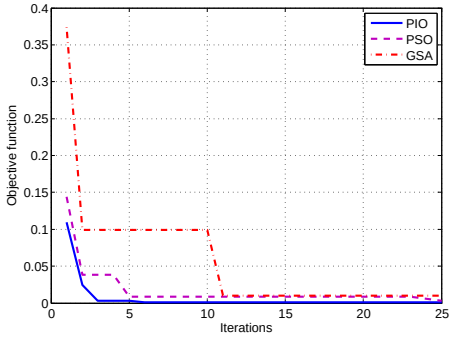

Figure 5. Comparative curves corresponding to best objective function

Downloaded by BEIHANG UNIVERSITY on April 28, 2018 | http://arc.aiaa.org | DOI: 10.2514/6.2017-4209

Further corresponding to the optimal bank angle $\sigma_0 = 71.6224\,\text{deg}$ obtained from PIO, the terminal errors in altitude, velocity and range-to-go are 1.2 km, 7 m/s, 0.0632 nmi respectively. These errors are within the tolerance limits according to Dukeman.[19] The corresponding entry trajectories are given in figures below. Figures 12, 13, 14 show that the path constraints are strictly met. The bank angle profile is shown in the figure 6. Series of bank reversals have minimized the terminal heading offset to 3.654 deg. This ensures that the vehicles terminal heading angle is aligned with the destination. After the initial descent, the vertical component of lift does not balance the gravitational and centrifugal forces, resulting in oscillations in flightpath angle as seen in figure 7. These variations in flightpath angle led to oscillations in the altitude profile observed in figure 8. Since the atmospheric density changes according to altitude, there are corresponding oscillations in the values of heat rate, dynamic pressure and load factors as in figures 12, 14, 13. Figures 10 and 9, show that the terminal conditions on velocity and range-to-go are accurately met. Figure 11, shows the variation of latitude with longitude.

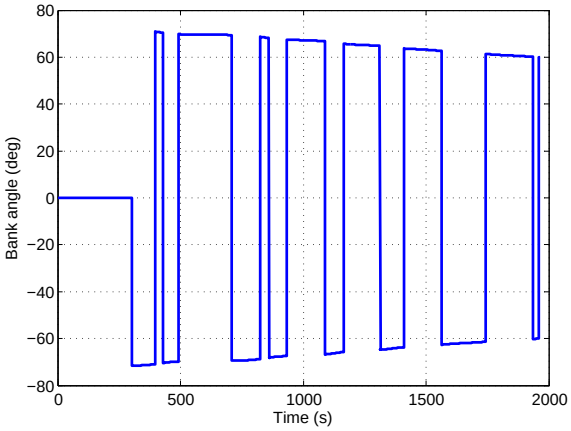

Figure 6. Bank angle profile

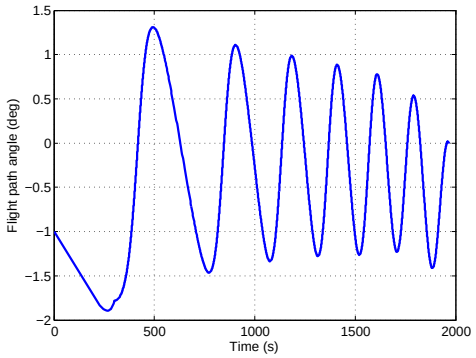

Figure 7. Variation of flightpath angle with time

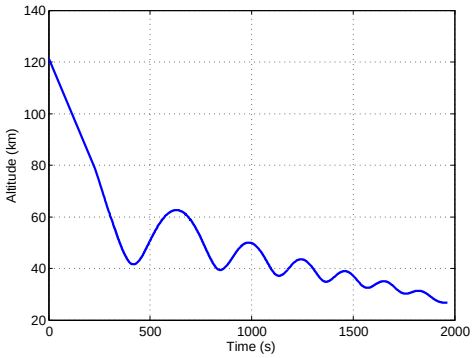

Figure 8. Variation of altitude with time

The optimal bank angle obtained using PSO has the terminal errors in altitude, velocity and range-to-go as 1.2067 km, 4.4175 m/s, 3.7883 nmi respectively. Although, errors are within the tolerance limit, PSO has taken many iterations to converge compared to PIO. The terminal errors obtained using GSA algorithm are 1.082 km, 3.8162 m/s, 32.61 nmi. Clearly, error in range-to-go is not within the tolerance limit. It can be concluded that PIO has faster convergence to the minimum objective function compared to PSO and GSA.

Downloaded by BEIHANG UNIVERSITY on April 28, 2018 | http://arc.aiaa.org | DOI: 10.2514/6.2017-4209

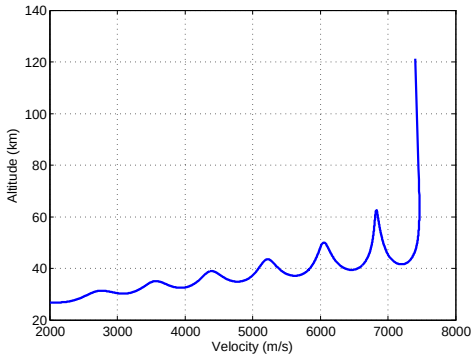

Figure 9. Altitude variation with respect to velocity

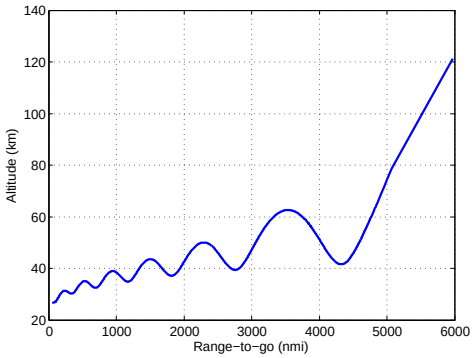

Figure 10. Variation of altitude with range-to-go

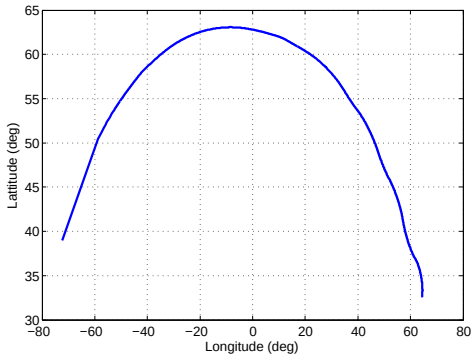

Figure 11. Latitude Vs Longitude

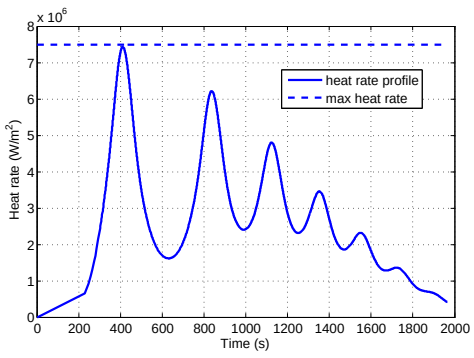

Figure 12. Variation of heat rate with time

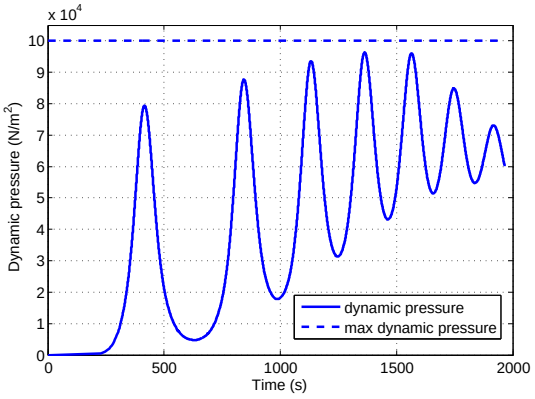

Figure 13. Variation of dynamic pressure with time

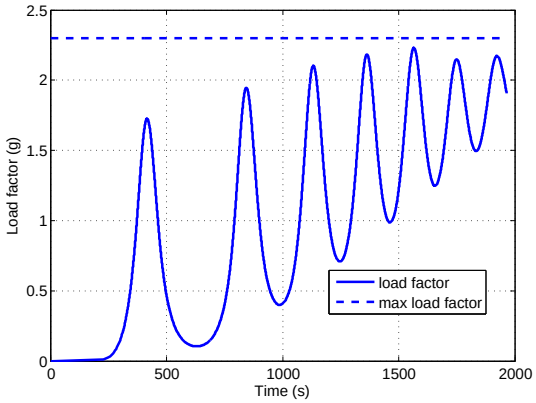

Figure 14. Variation of load factor with time

VI. Conclusion

The entry trajectory that satisfies the path and terminal constraints has been generated using PIO. The performance comparison show that the mean of objective function is minimum for PIO when compared to PSO and GSA. It also converges quickly in less number of iterations. It can be concluded that, PIO is better than PSO and GSA in solving the trajectory optimization problem. However, more studies are necessary to establish the performance of PIO in different cases.

Downloaded by BEIHANG UNIVERSITY on April 28, 2018 | http://arc.aiaa.org | DOI: 10.2514/6.2017-4209

References

[1]Pontryagin, L.S., Boltyanskii, V., Gamkrelidze, R., Mischenko, E., *The Mathematical Theory of Optimal Processes*. Wiley Interscience, New York City, NY, 1962.

[2]Betts, J.T., *Practical Methods for Optimal Control Using Nonlinear Programming*, Society for Industrial and Applied Mathematics Press, 2001.

[3]Tian, B. and Qun Zong.,"Optimal guidance for reentry vehicles based on indirect Legendre pseudospectral method", *Acta Astronautica*, Vol. 68, Iss. 7, pp. 1176-1184.

[4]Jorris, T. R., Schulz, C. S., Friedl, F. R., and Rao, A. V.,"Constrained trajectory optimization using pseudospectral methods", *Proceedings of the AIAA Atmospheric Flight Mechanics Conference and Exhibit*, 2008.

[5]Karthikeyan Kalirajan and Ashok Joshi.,"Optimal Gliding Guidance for Long Range Hypersonic vehicles with Impact angle Constraints using Pseudospectral Method", *AIAA Atmospheric Flight Mechanics Conference*, 2016.

[6]Cai, W. W., Zhu, Y. W., Yang, L. p., and Zhang, Y. W.,"Optimal guidance for hypersonic reentry using inversion and receding horizon control", *IET Control Theory and Applications*, Vol. 9, No. 9, 2015, pp. 1347-1355.

[7]Deb, K., "An introduction to genetic algorithms", *Sadhana*, Vol. 24, No. 4, 1999, pp. 293-315.

[8]Eberhart, R. and Kennedy, J., "A new optimizer using particle swarm theory", *Micro Machine and Human Science*, 1995.

[9]Dorigo, M., Birattari, M., and Stutzle, T., "Ant colony optimization", *IEEE Computational Intelligence Magazine*, Vol. 1, No. 4, 2006, pp. 28-39.

[10]Rahimi, A., Dev Kumar, K., and Alighanbari, H., "Particle Swarm Optimization Applied to Spacecraft Reentry Trajectory", *Journal of Guidance, Control, and Dynamics*, Vol. 36, No. 1, 2013, pp. 307-310. doi: 10.2514/1.56387

[11]Duan, H., and Qjao, P., "Pigeon-inspired optimization: a new swarm intelligence optimizer for air robot path planning", *International Journal of Intelligent Computing and Cybernetics*, Vol. 7, Iss. 1, 2014, pp. 24-37. doi: 10.1108/IJICC-02-2014-0005

[12]Zhao, J. and Zhou, R., "Particle swarm optimization applied to hypersonic reentry trajectories", *Chinese Journal of Aeronautics*, Vol. 28, Iss. 3, 2015, pp. 822-831. doi: 10.1016/j.cja.2015.04.007

[13]Zhao, J. and Zhou, R.,"Pigeon-inspired optimization applied to constrained gliding trajectories", *Nonlinear Dynamics*, Vol. 82, Iss. 4, 2015, pp. 1781-1795. doi: 10.1007/s11071-015-2277-9

[14]Lu, P., "Entry Guidance: A Unified Method", *Journal of Guidance, Control, and Dynamics*, Vol. 37, No. 3, 2014, pp. 713-728. doi:10.2514/1.62605

[15]Shen, Z. and Lu, P., "Dynamic Lateral Entry Guidance Logic", *Journal of Guidance, Control, and Dynamics*, Vol. 27, No. 6, 2004, pp. 949-959. doi:10.2514/1.8008

[16]Zhang, S. and Duan, H., "Gaussian pigeon-inspired optimization approach to orbital spacecraft formation reconfiguration", *Chinese Journal of Aeronautics*, Vol. 28, Iss. 1, 2015, pp. 200-205. doi: 10.1016/j.cja.2014.12.008

[17]Phillips, T. H., A common aero vehicle (CAV) model, description, and employment guide, Schafer Corporation for Air Force Research Laboratory (AFRL) and Air Force Space Command (AFSPC), 2003.

[18]Rashedi, E., Nezamabadi-pour, H., Saryazdi, S., "GSA: A Gravitational Search Algorithm", *Information Sciences*, 2009, pp. 2232-2248.

[19]Dukeman, G.,"Profile-Following Entry Guidance Using Linear Quadratic Regulator Theory", *AIAA Guidance, Navigation, and Control Conference and Exhibit*, 2002.

[20]Yu, W., Chen, W.,"Entry guidance with real-time planning of reference based on analytical solutions", *Advances in Space Research*, Vol. 55, Iss. 9, 2015, pp. 2325-2345.

[21]Lu, P.,"Entry Guidance Using Time-Scale Separation in Gliding Dynamics", *Journal of Spacecraft and Rockets*, Vol. 52, No. 4, 2015, pp. 1253-1258.

Downloaded by BEIHANG UNIVERSITY on April 28, 2018 | http://arc.aiaa.org | DOI: 10.2514/6.2017-4209